

Acta Crystallographica Section D

**Biological
Crystallography**

ISSN 0907-4449

Dynamic light-scattering analysis of full-length human RPA14/32 dimer: purification, crystallization and self-association

Jeff E. Habel, Jeffrey F. Ohren and Gloria E. O. Borgstahl

Copyright © International Union of Crystallography

Author(s) of this paper may load this reprint on their own web site provided that this cover page is retained. Republication of this article or its storage in electronic databases or the like is not permitted without prior permission in writing from the IUCr.

Dynamic light-scattering analysis of full-length human RPA14/32 dimer: purification, crystallization and self-association

Jeff E. Habel, Jeffrey F. Ohren
and Gloria E. O. Borgstahl*

University of Toledo, Department of Chemistry,
2801 West Bancroft Street, Toledo, OH 43606,
USA

Correspondence e-mail:
gborgst@uoft02.utoledo.edu

Received 21 June 2000
Accepted 25 October 2000

Replication protein A (RPA) is a single-stranded DNA-binding protein involved in all aspects of eukaryotic DNA metabolism. A soluble heterodimeric form of RPA is composed of 14 and 32 kDa subunits (RPA14/32). Dynamic light-scattering (DLS) analysis was used to improve the purification, stabilization and crystallization of RPA14/32. Increasing the concentration of reducing agent in the last stage of purification diminished the size of a secondary peak in the anion-exchange chromatograph and promoted a single species in solution. This resulted in decreased polydispersity in the purified protein and enhanced the crystallization time from 9–12 months to 6 d. With this homogeneous preparation, the reversible association of RPA14/32 into a dimer of dimers was demonstrated by DLS. Four different crystal forms of RPA14/32 were obtained for structure determination and complete diffraction data were collected using synchrotron radiation for three of them. Data to 2.4 Å resolution was collected from hexagonal crystals ($P3_2$ or $P3_1$; $a = b = 63.0$, $c = 272.6$ Å) and to 2.2 and 1.9 Å resolution from two orthorhombic crystal forms (both $P2_12_12_1$; form I, $a = 61.4$, $b = 75.2$, $c = 131.6$ Å; form II, $a = 81.8$, $b = 140.4$, $c = 173.1$ Å).

1. Introduction

Replication protein A (RPA) is a single-stranded DNA-binding protein that has been implicated in all aspects of eukaryotic DNA metabolism, including replication, transcription, recombination and repair (for reviews, see Wold, 1997; Iftode *et al.*, 1999). The three subunits of RPA are designated RPA14, RPA32 and RPA70 according to their apparent molecular weights. RPA70 contains the primary ssDNA-binding site and interacts with several proteins, including P53 (Dutta *et al.*, 1993; He *et al.*, 1993; Li & Botchan, 1993) and XPA (Lee & Kim, 1995; Li *et al.*, 1995; Matsuda *et al.*, 1995). RPA32 is phosphorylated in a cell-cycle-dependent manner (Din *et al.*, 1990; Fang & Newport, 1993) during apoptosis (Treuner *et al.*, 1999) and in response to UV light (Carty *et al.*, 1994) and ionizing radiation (Liu & Weaver, 1993; Boubnov & Weaver, 1995; Fried *et al.*, 1996). *In vitro*, RPA32 is phosphorylated by ATM kinase (Gately *et al.*, 1998), cdc2 kinase (Dutta & Stillman, 1992) and DNA-dependent protein kinase (Brush *et al.*, 1994; Boubnov & Weaver, 1995). RPA32 contains a weak ssDNA-binding site (Bochkareva *et al.*, 1998) and its C-terminal domain interacts with several proteins, including RAD52 (Park *et al.*, 1996) and XPA. RPA14 plays a structural role in heterotrimer assembly and stability (Henricksen *et al.*, 1994). RPA is known to exist in two soluble forms: the heterotrimer and the RPA14/32 heterodimer

(Henricksen *et al.*, 1994). The RPA heterotrimer is extremely stable (Fairman & Stillman, 1988; Wold & Kelly, 1988; Brill & Stillman, 1991) and its roles in DNA metabolism are well known. Interestingly, the separation of the RPA14/32 dimer from RPA70 is promoted by hyperphosphorylation of RPA32 both *in vitro* (Treuner, Findeisen *et al.*, 1999) and in cells undergoing apoptosis (Treuner, Okuyama *et al.*, 1999). These studies suggest a physiological role for the RPA14/32 dimer.

Owing to the multidimensional role RPA plays in DNA metabolism, it is of great interest to understand the structure in atomic detail. An NMR solution structure of the N-terminal RPA70 domain (Jacobs *et al.*, 1999) and crystal structures at moderate resolution of proteolytic core fragments of RPA70 (Bochkarev *et al.*, 1997) and RPA14/32 (Bochkarev *et al.*, 1999) have been reported. Unfortunately, the intact full-length holoenzyme is very difficult to purify and structural data remain elusive. Here, we demonstrate the utility of using dynamic light-scattering (DLS) analysis in improving the purification, stabilization and crystallization of full-length recombinant human RPA14/32 dimer. Complete diffraction data from orthorhombic and hexagonal crystals are reported.

2. Experimental

2.1. Expression and purification

RPA14 and RPA32 subunits were co-expressed from a single pET16 plasmid (Novagen). A 6×His tag followed by a thrombin cleavage site was placed at the N-terminus of RPA14. BL21(DE3) cells (Novagen) were transformed and 8 l of Terrific Broth containing 100 µg ml⁻¹ ampicillin was inoculated with an 8 ml starter culture and rested at room temperature overnight in a laboratory fermentor (Virtis). The next morning the culture was grown (300 rev min⁻¹, 310 K, 15 l O₂ min⁻¹) to an OD₆₀₀ of 4.0–5.0 (4.5–5 h), induced with 1 mM IPTG and grown for another 3.5–4 h. The cells were harvested by centrifugation (10 000 rev min⁻¹, 277 K, 10 min) and the cell pellet was resuspended in four volumes of lysis buffer (30 mM HEPES pH 7.8, 200 mM KCl) supplemented with 4–10 mM imidazole and 1 mM DTT.

For preparation *A*, the cells were lysed by sonication, centrifuged (15 000 rev min⁻¹, 277 K, 30 min) and the supernatant was passed through a 0.20 µm filter. The clarified lysate was loaded onto a 1.67 ml MC/M Ni²⁺ affinity column (PerSeptive Biosystems) equilibrated with lysis buffer with 4 mM imidazole. The column was washed with 15 column volumes (CV) of lysis buffer with 60 mM imidazole and the protein eluted with a 60–1000 mM, 20 CV imidazole gradient using the BioCAD Sprint. For preparations *B–G*, the cells were lysed by three passes through a French pressure cell (SLM-Aminco). The lysed cells were centrifuged and supernatant was passed through 5–10 ml of Cellular Debris Remover resin (Whatman) in a 60 ml syringe. The clarified lysate was loaded onto a 5 ml Ni-NTA Superflow column (Qiagen) equilibrated with lysis buffer with 10 mM imidazole. The column was washed with 10 CV of lysis buffer with 10 mM imidazole and the protein was eluted with a 10–500 mM 20 CV

Table 1

Interpretation and use of the statistical parameters calculated by *Dynamics* 4.0.

Parameter	Interpretation†
Baseline	
0.977–1.002	Monomodal distribution
1.003–1.005	Bimodal distribution, use <i>DynaLS</i>
>1.005	Bimodal/multimodal distribution, use <i>DynaLS</i>
Sum of squares (SOS)	
1.000–5.000	Low noise, negligible error
5.000–20.000	Background error owing to noise, low protein concentration or a small amount of polydispersity
>20.000	High noise/error owing to high polydispersity in size distribution (aggregation), irregular solvent
Polydispersity	Note: this parameter should be used for monomodal distributions only
$C_p/R_H < 15\%$	Monodisperse solution, very likely to crystallize
$C_p/R_H < 30\%$	A moderate amount of polydispersity, more likely to crystallize
$C_p/R_H > 30\%$	A significant amount of polydispersity, less likely to crystallize

† Adapted from the DynaPro-801 Operator Manual, Protein Solutions Inc.

imidazole gradient using a Bio-Logic LP system (Bio-Rad). For preparations *A–G*, the pooled fractions were diluted five times with 30 mM HEPES pH 7.8 and varying amounts of fresh DTT was added. The diluted protein was loaded onto a 1.67 ml POROS HQ/M strong anion-exchange column (PerSeptive Biosystems). The column was washed with 10 CV of 30 mM HEPES pH 7.8 containing DTT and 10 mM KCl. For preparation *A*, the protein was eluted with a 10–1000 mM KCl 10 CV gradient. For preparations *B–G*, a gradient from 10–700 mM KCl over 40 CV was used. All column fractions were analyzed by SDS–PAGE (Pharmacia LKB PhastSystem) and those HQ column fractions of sufficient concentration were also analyzed by DLS. Pooled fractions were concentrated with a Centriprep YM-10 (Amicon). Protein concentration was determined using the Bradford Protein Assay (BioRAD) with BSA as the standard.

2.2. Dynamic light-scattering analysis

DLS was carried out using a DynaPro-801 molecular-sizing instrument equipped with a microsampler (Protein Solutions). A 50 µl sample was passed through a filtering assembly containing a 0.02 µm filter into a 12 µl chamber quartz cuvette. The data were analyzed using the *Dynamics* 4.0 and *DynaLS* software as described by Moradian-Oldak *et al.* (1998). Interpretation of the statistical parameters generated by the *Dynamics* 4.0 software is summarized in Table 1.

2.3. Crystallization

All crystallization was performed at 293 K using vapor-diffusion methods with hanging or sitting drops. Drop volumes of 4 µl (by mixing equal volumes of protein and reservoir solutions) and reservoir volumes of 500 µl were used. Initial screening was performed with Hampton Research Crystal Screens 1 and 2 (Jancarik & Kim, 1991).

Table 2

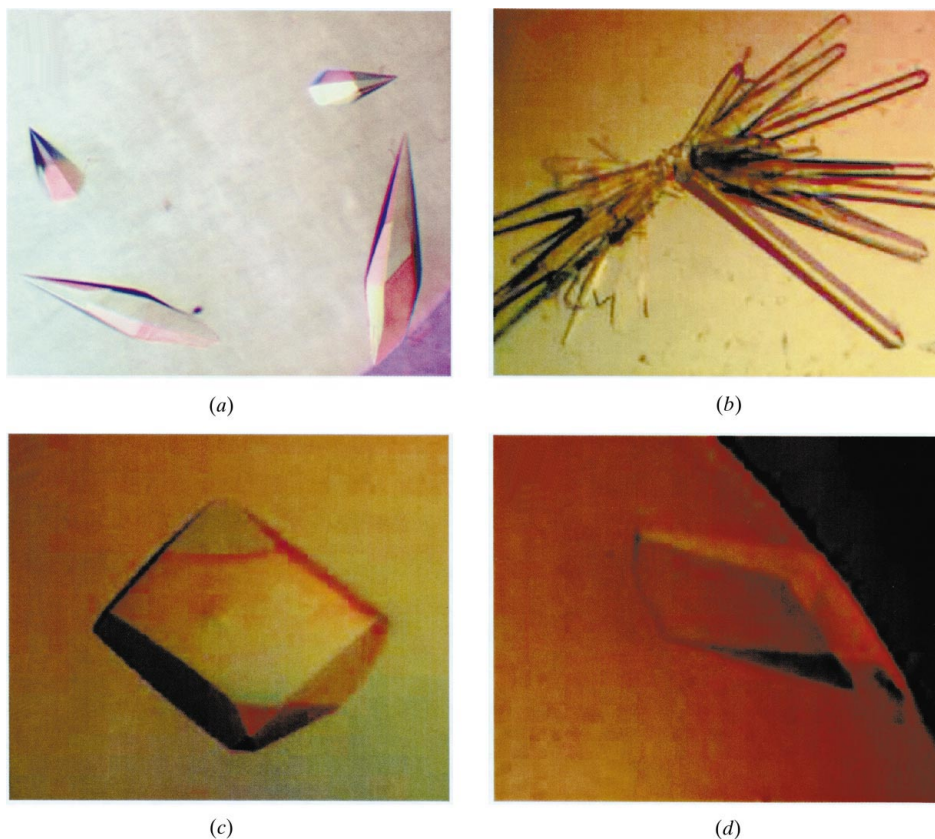
Dynamic light-scattering data and resultant crystallization time.

 Data with a monomodal distribution was analyzed using *Dynamics* 4.0 and multimodal data with *DynaLS*, with percentages of peak area given in parentheses. The concentration of DTT used in the HQ buffer system is given. Crystallization condition I was used for each preparation and monitored weekly.

Preparation	Concentration (mg ml ⁻¹)	R_H (nm)	MW (kDa)	C_P (nm)	C_P/R_H (%)	Base-line	SOS error	DTT (mM)	Time (d)
A	5	3.1 (77) 1090 (23)	45.0	NA	NA	1.047	1.400	0	270–360
B	1–2	3.41	56.8	1.1	33.1	1.001	6.065	0	28
C	1–2	3.39	56.0	0.9	25.7	1.000	4.550	1	28
D	1–2	3.49	59.9	0.7	20.8	1.001	1.397	5	14
E	10	3.39	56.1	0.6	18.3	1.000	1.363	10	6
F	10	3.60	64.9	0.6	17.5	1.000	0.848	10	6
G	13	4.13	90.3	0.6	14.5	1.000	0.666	10	NA

2.4. Data collection

Single crystals were immersed in cryoprotectant (either the reservoir solution with 30% glycerol or paratone-N oil) for 3 s, mounted in a cryoloop and immediately placed in a 100 K nitrogen-gas stream. Diffraction data were collected on hexagonal (Fig. 1*a*) and orthorhombic crystal form II (Fig. 1*d*)


Figure 1

Crystals of RPA14/32. (a) Hexagonal crystals grown from preparation A with a precipitating solution of 0.1 M bicine pH 9.0, 10% acetonitrile and 20% saturated ammonium sulfate. The largest crystal was 90 × 150 μm. (b) Monoclinic crystals grown from preparation E with 10% dioxane, 0.1 M MES pH 6.5 and 37% saturated ammonium sulfate. The largest crystal was 44 × 440 μm. (c) Orthorhombic crystal form I grown from preparation P1 with 0.1 M MES pH 6.3, 5% saturated ammonium sulfate and 26% PEG MME 5000 (242 × 275 μm). (d) Orthorhombic crystal form II grown from preparation P1 with 10% dioxane, 0.1 M MES pH 6.5 and 39% saturated ammonium sulfate (132 × 220 μm).

at Stanford Synchrotron Radiation Laboratory beamline 7-1 with a MAR345 detector at a wavelength of 1.08 Å. Low-resolution (LR) and high-resolution (HR) passes were designed using *MOSFLM/STRATEGY*. For hexagonal crystals, 28 HR images were collected at a crystal-to-detector distance (XTD) of 300 mm, $\Delta\varphi = 2^\circ$ using the 345 mm plate (edge = 2.09 Å), 30 LR images were collected at an XTD of 350 mm and 58 LR images were collected at an XTD of 300 mm using the 180 mm plate (edge = 3.72–4.3 Å). For orthorhombic form II crystals, 365 HR images were collected at an XTD of 225 mm, $\Delta\varphi = 0.25^\circ$ (0.5° for 20 images) using the 300 mm plate (edge = 1.86 Å) and 366 LR images were collected at an XTD of 240 mm, $\Delta\varphi = 0.5^\circ$ (1.0° for 48 images) using the 180 mm plate (edge = 3.03 Å). Images were integrated with *MOSFLM* (Powell, 1999) and scaled using *SCALA* and the *CCP4i* graphical interface (Collaborative Computational Project, Number 4, 1994). The HR data

from the orthorhombic crystals were difficult to integrate because all the data were recorded as partial reflections. A pre-release of a new version of *MOSFLM* was provided by Dr Harry Powell to integrate these images using the POSTREF MULTI keyword.

Diffraction data were collected from orthorhombic crystal form I (Fig. 1*c*) at beamline 17-ID in the facilities of the Industrial Macromolecular Crystallography Association Collaborative Access Team (IMCA-CAT) at the Advanced Photon Source (APS). 180 images were collected at a crystal-to-detector distance of 120 mm with $\Delta\varphi = 1^\circ$, $\lambda = 1.2$ Å and using the MARCCD detector. Data were processed using the *HKL2000* program suite (Otwinowski & Minor, 1996).

3. Results and discussion

RPA14/32 was overexpressed in *Escherichia coli* and up to 15 mg of pure protein was obtained from a liter of culture. Since monodispersity is thought to be predictive of crystallizability (Zulauf & D'Arcy, 1992; Ferre-D'Amare & Burley, 1997), DLS was used to examine all preparations of RPA14/32. Initial

purifications were multimodal (baseline 1.047) and polydisperse (Table 2, preparation *A*) and did not crystallize unless organics were added to the crystallization setup. After 9–12 months, hexagonal crystals grew from solutions that contained 20–30% saturated ammonium sulfate, 0.1 M HEPES, Tris or bicine pH 7–9 and 6–10% organic solvent (acetonitrile, 2-propanol or methanol). Although of diffraction quality, these crystals were difficult to reproduce (Fig. 1*a*).

Preparation *B* was monomodal (baseline 1.001, Table 2) but was significantly polydisperse ($C_p/R_H = 33.1$). Initial crystallization screens produced microcrystals within a month. Grid-screen optimization resulted in the following crystallization condition that produced monoclinic diffraction-quality crystals (Fig. 1*b*): 10% dioxane, 0.1 M MES pH 5.7–6.5 and 34–41% saturated ammonium sulfate (condition I). Prepara-

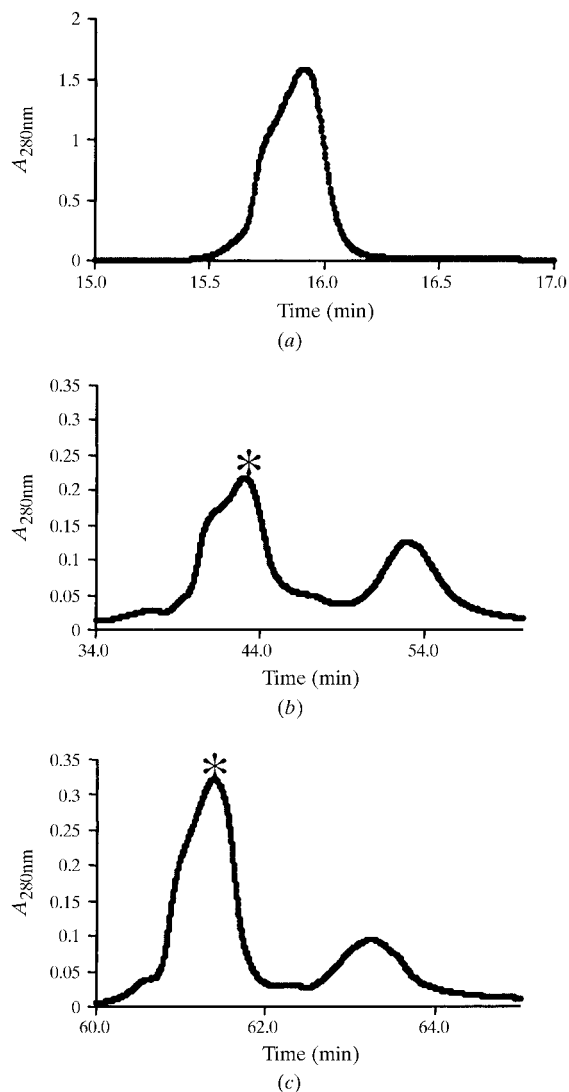


Figure 2
Representative chromatograms of RPA14/32 elution at ~ 300 mM KCl from the HQ anion-exchange column. (a) Preparation *A*, (b) preparation *B*, (c) preparation *C*. SDS-PAGE analysis showed that all peaks are composed of hRPA14/32 dimer (data not shown). For preparations *B–G*, the fractions corresponding to the peak indicated with an asterisk (*) were collected.

Table 3

Dynamic light-scattering data for chromatography peaks *P* and *P1*.

Preparation	Concentration (mg ml ⁻¹)	R_H (nm)	MW (kDa)	C_p (nm)	C_p/R_H (%)	Baseline error	SOS
<i>P</i>	8.2	4.12	89.7	0.9	22.8	1.001	1.201
<i>P1</i>	8.5	3.62	65.5	0.9	23.7	1.001	1.431
<i>P + P1</i>	8.35	3.9 (91) 1170 (6.6)	78.5	NA	NA	1.005	2.841

tion *B* was significantly less polydisperse and crystallized in less time than preparation *A*. The differences between these preparations, the lysis method and the type of nickel affinity matrix used, do not account for the overall improvement in polydispersity. The elution profiles from the HQ anion-exchange column (Figs. 2*a* and 2*b*) show that in preparation *B*, where a shallower salt gradient was used, two peaks were separated, whereas in preparation *A* the protein eluted as one peak. In both preparations, analysis by SDS-PAGE indicated that all the peaks contained only RPA14/32. The lack of separation of these peaks in preparation *A* probably contributed greatly to the polydispersity of the early RPA14/32 samples (see below).

The primary sequence of RPA14/32 contains four cysteine residues (two in each subunit) and the structure of the proteolytic core of RPA14/32 had free cysteines (Bochkarev *et al.*, 1999). These observations suggested the need for a reducing environment during protein purification. The effect of varying the concentration of dithiothreitol (DTT) in the HQ buffer system was monitored by DLS and crystallization time. In preparations *B–G*, as the DTT concentration was increased, polydispersity (C_p/R_H) and the time for crystal formation systematically decreased (Table 2). A DTT effect was also seen in the elution profiles. When fresh 1 mM DTT was added during the dilution of the protein sample and added to the HQ buffer system, the first peak increased and the second peak decreased (Figs. 2*b* and 2*c*). With 10 mM DTT, the second peak nearly disappears (data not shown). This suggests that the reduction of disulfide bond(s) is involved in converting the second peak into the first peak.

As frequently happens in science, an interesting observation on RPA14/32 came from careful analysis of a fortuitous mistake. Early in this work, the ionic strength of the protein sample was not reduced by dilution before loading onto the HQ column. The standard HQ protocol was run and a fraction of the protein sample was found to bind to the column (fraction *P*, Table 2). The flowthrough from this column was then diluted and reloaded onto the HQ column. The protein fraction *P1* was eluted from the column. When analyzed by DLS (Table 3), fractions *P* and *P1* were monomodal (baseline 1.001) with moderate polydispersity (C_p/R_H 23%). However, when the two fractions were mixed together, the solution became multimodal (baseline 1.005) with 7% high-molecular-weight aggregates. The molecular weight of fraction *P* (90 kDa) corresponded to that of a dimer of dimers, whereas fraction *P1* was closer to that of a single dimer.

Table 4

Dynamic light-scattering data collected at various time points after the addition of acetonitrile to *P* + *P1* mixture.

Time (h)	R_H (nm)	MW (kDa)	Baseline error	SOS
0	3.61 (77.5) 1340 (8.7)	65.1	1.010	1.837
1	3.84 (94.4) 1310 (4.4)	75.6	1.003	1.539
3	4.02 (96.4) 1270 (1.9)	84.5	1.001	1.459

Table 5

Dynamic light-scattering data on the dilution of preparation *G*.

Line No.	Concentration (mg ml ⁻¹)	R_H (nm)	MW (kDa)	C_p (nm)	C_p/R_H (%)	Baseline error	SOS
1	13	4.13	90.3	0.6	14.5	1.000	0.677
2	6.5	3.52 (77.7) 30.1 (3.3) 986 (18.3)	61.2 11200	NA	NA	1.022	5.211
3	6.5	3.52 (87.4) 1330 (6.7)	61.2	NA	NA	1.005	0.881
4	6.5	3.69	68.5	0.6	16.6	1.000	0.522

Crystallization conditions were screened and optimized for preparation *P1*. Large chunky crystals (Fig. 1c) were obtained from solutions containing 0–5% saturated ammonium sulfate, 0.1 M MES pH 5.9–6.5 and 16–36% PEG MME 5000 (condition II). These crystals were extremely sensitive and cracked easily when cryoprotected with glycerol. Diffraction data of reasonable quality was obtained using paratone-N oil as a cryoprotectant. Preparations *B–G* will not crystallize under condition II but preparation *P1* will crystallize under condition I in an orthorhombic space group (Fig. 1d).

The different oligomerization state of the protein fractions *P* and *P1* may explain the multimodality and polydispersity of preparation *A*. Since crystals were obtained when 6–10% organic solvent was added to preparation *A*, it was postulated that acetonitrile would reduce the polydispersity of the *P* + *P1* mixture. Acetonitrile was added to the *P* + *P1* mixture to a final concentration of 6%, incubated at 277 K for 3 h and monitored periodically by DLS (Table 4). Incubation with acetonitrile caused the amount of non-aggregated RPA14/32 to increase from 78 to 96% and the solution becomes monomodal. Interestingly, the molecular weight of the non-aggregated species continues to increase until it is roughly the size of a dimer of dimers.

It was noted that as the protein concentration increased, the molecular weight increased (Table 2) and at 13 mg ml⁻¹ (preparation *G*) it was consistent with a dimer of dimers in solution. Therefore, this apparent self-association of the dimer was analyzed by dilution followed by DLS. Samples of preparation *G* (Table 5, row 1) were diluted with an equal volume of the following buffers: 30 mM HEPES pH 7.8 buffer (row 2), 30 mM HEPES pH 7.8 and 200 mM KCl (row 3) or 30 mM HEPES pH 7.8, 200 mM KCl and 10 mM DTT (row 4). Dilution with buffer alone produced a smaller molecular

Table 6

Data-collection statistics.

	Orthorhombic form I	Orthorhombic form II	Hexagonal
Beamline	APS 17-ID	SSRL 7-1	SSRL 7-1
Detector	MAR CCD	MAR345	MAR345
Temperature (K)	100	100	100
Wavelength (Å)	1.2	1.08	1.08
Space group	$P2_12_12_1$	$P2_12_12_1$	$P3_2$ (or $P3_1$)
Unit-cell parameters (Å)	$a = 61.4,$ $b = 75.2,$ $c = 131.7$	$a = 81.8,$ $b = 140.4,$ $c = 173.1$	$a = b = 63.0,$ $c = 272.6$
Heterodimers in the asymmetric unit	1	3–5	2–3
V_M (Å ³ Da ⁻¹)	3.17	3.42–2.05	3.25–2.17
Solvent content (%)	61	64–40	62–43
Resolution (Å)	2.20	1.86	2.40
No. of measured reflections	181370	820454	141010
No. of unique reflections	31207	158549	43885
Completeness (%)	98.2 (97.9)	95.6 (81.4)	92.7 (91.9)
$I/\sigma(I)$	18.3 (2.5)	9.3 (1.0)	4.5 (1.0)
Multiplicity	5.8	5.2 (3.3)	3.2 (2.0)
R_{merge}^\dagger (%)	8.9	6.0	11.7

$$\dagger R_{\text{merge}} = \sum_{hkl} (|I_{hkl}| - I_{hkl}) / \sum_{hkl} I_{hkl}$$

weight species in addition to large aggregates. Dilution with buffer and salt also produced large-molecular-weight aggregates, but more of the protein sample remains as the single dimer as indicated by an increase in the peak area (from 78 to 87%) associated with the 61 kDa species. Addition of DTT produced a monomodal solution and completely disrupted the large-molecular-weight aggregates. Therefore, the large aggregates of RPA14/32 are probably a consequence of inappropriate disulfide-bond formation and the dimer of dimers appears to be a reversible association. The physiological roles of the RPA14/32 dimer of dimers and the solvent-accessible cysteines on the surface of the molecule are unknown. The possibility of a RPA14/32 dimer of dimers was also suggested by Bochkarev *et al.* (1999).

Three complete sets of cryocooled synchrotron diffraction data have been collected for structure determination (Table 6). Space groups were assigned by autoindexing, comparing R_{merge} values for space groups within the indicated Laue group and by observed systematic absences. The hexagonal crystals (Fig. 1a) diffracted to 2.4 Å resolution, with space group $P3_2$ (or $P3_1$) and unit-cell parameters $a = b = 63.0$, $c = 272.6$ Å. The orthorhombic crystal form I (Fig. 1c) diffracted to 2.2 Å resolution, with space group $P2_12_12_1$ and unit-cell parameters $a = 61.4$, $b = 75.2$, $c = 131.7$ Å. The orthorhombic crystal form II (Fig. 1d) diffracted to 1.9 Å resolution with space group $P2_12_12_1$ and unit-cell parameters $a = 81.8$, $b = 140.4$, $c = 173.1$ Å. Interestingly, solvent-content analysis (Matthews, 1968) indicates several heterodimers in the asymmetric unit of the orthorhombic crystal form II and hexagonal unit cells. Solution of the phase problem using coordinates of a proteolytic fragment of RPA14/32 (containing intact RPA14 and 60% of RPA32; PDB code 1quq) is in progress.

We would like to thank Dr Marc Wold of the University of Iowa for providing the RPA14/32 expression plasmid, Dr

Harry Powell at the MRC Centre in Cambridge, England for the pre-release of *MOSFLM* and many helpful discussions on data processing, and Mr Vinay Gupta for technical assistance in crystal growth. Grants from the Ohio Cancer Research Associates, Inc. and the US Army Medical Research and Materiel Command DAMD17-98-1-8251 supported this work. The IMCA-CAT facilities are supported by the companies of the IMCA through a contract with Illinois Institute of Technology (IIT), executed through IIT's Center for Synchrotron Radiation Research and Instrumentation. APS and SSRL are supported by the US Department of Energy, Basic Energy Sciences (BES), Office of Science. The Biotechnology Program at SSRL is supported by the National Institutes of Health, National Center for Research Resources, Biomedical Technology Program and the Department of Energy, Office of Biological and Environmental Research.

References

- Bochkarev, A., Bochkareva, E., Frappier, L. & Edwards, A. M. (1999). *EMBO J.* **18**, 4498–4504.
- Bochkarev, A., Pfuetzner, R. A., Edwards, A. M. & Frappier, L. (1997). *Nature (London)*, **385**, 176–181.
- Bochkareva, E., Frappier, L., Edwards, A. M. & Bochkarev, A. (1998). *J. Biol. Chem.* **273**, 3932–3936.
- Boubnov, N. V. & Weaver, D. T. (1995). *Mol. Cell. Biol.* **15**, 5700–5706.
- Brill, S. J. & Stillman, B. (1991). *Genes Dev.* **5**, 1589–1600.
- Brush, G. S., Anderson, C. W. & Kelly, T. J. (1994). *Proc. Natl Acad. Sci. USA*, **91**, 12520–12524.
- Carty, M. P., Zernik-Kobak, M., McGrath, S. & Dixon, K. (1994). *EMBO J.* **13**, 2114–2123.
- Collaborative Computational Project, Number 4 (1994). *Acta Cryst.* **D50**, 760–763.
- Din, S.-U., Brill, S. J., Fairman, M. P. & Stillman, B. (1990). *Genes Dev.* **4**, 968–977.
- Dutta, A., Ruppert, J. M., Aster, J. C. & Winchester, E. (1993). *Nature (London)*, **365**, 79–82.
- Dutta, A. & Stillman, B. (1992). *EMBO J.* **11**, 2189–2199.
- Fairman, M. P. & Stillman, B. (1988). *EMBO J.* **7**, 1211–1218.
- Fang, F. & Newport, J. W. (1993). *J. Cell Sci.* **106**, 983–994.
- Ferre-D'Amare, A. R. & Burley, S. K. (1997). *Methods Enzymol.* **276**, 157–166.
- Fried, L. M., Koumenis, C., Peterson, S. R., Green, S. L., Zijl, P. V., Turner, J. A., Chen, D. J., Fishel, R., Giaccia, A. J., Brown, J. M. & Kirchgessner, C. U. (1996). *Proc. Natl Acad. Sci. USA*, **93**, 13825–13830.
- Gately, D. P., Hittle, J. C., Chan, G. K. T. & Yen, T. J. (1998). *Mol. Biol. Cell.* **9**, 2361–2374.
- He, Z., Brinton, B. T., Greenblatt, J., Hassell, J. A. & Ingles, C. J. (1993). *Cell*, **73**, 1223–1232.
- Henricksen, L. A., Umbricht, C. B. & Wold, M. S. (1994). *J. Biol. Chem.* **269**, 11121–11132.
- Iftode, C., Daniely, Y. & Borowiec, J. A. (1999). *Crit. Rev. Biochem. Mol. Biol.* **34**, 141–180.
- Jacobs, D. M., Lipton, A. S., Isern, N. G., Daughdrill, G. W., Lowry, D. F., Gomes, X. & Wold, M. S. (1999). *J. Biomol. NMR*, **14**, 321–331.
- Jancarik, J. & Kim, S.-H. (1991). *J. Appl. Cryst.* **24**, 409–411.
- Lee, S. H. & Kim, D. K. (1995). *J. Biol. Chem.* **270**, 12801–12807.
- Li, L., Lu, X., Peterson, C. A. & Legerski, R. J. (1995). *Mol. Cell. Biol.* **15**, 5396–5402.
- Li, R. & Botchan, M. R. (1993). *Cell*, **73**, 1207–1221.
- Liu, V. F. & Weaver, D. T. (1993). *Mol. Cell. Biol.* **13**, 7222–7231.
- Matsuda, T., Saijo, M., Kuraoka, I., Kobayashi, T., Nakatsu, Y., Nagai, A., Enjoji, T., Masutani, C., Sugawara, K., Hanaoka, F., Yasui, A. & Tanaka, K. (1995). *J. Biol. Chem.* **270**, 4152–4157.
- Matthews, B. W. (1968). *J. Mol. Biol.* **33**, 491–497.
- Moradian-Oldak, J., Leung, W. & Fincham, A. G. (1998). *J. Struct. Biol.* **122**, 320–327.
- Otwinowski, Z. & Minor, W. (1996). *Methods Enzymol.* **276**, 307–326.
- Park, M. S., Ludwig, D. L., Stigger, E. & Lee, S. H. (1996). *J. Biol. Chem.* **271**, 18996–19000.
- Powell, H. R. (1999). *Acta Cryst.* **D55**, 1690–1695.
- Treuner, K., Findeisen, M., Strausfeld, U. & Knippers, R. (1999). *J. Biol. Chem.* **274**, 15556–15561.
- Treuner, K., Okuyama, A., Knippers, R. & Fackelmayer, F. O. (1999). *Nucleic Acids Res.* **27**, 1499–1504.
- Wold, M. S. (1997). *Annu. Rev. Biochem.* **66**, 61–91.
- Wold, M. S. & Kelly, T. (1988). *Proc. Natl Acad. Sci. USA*, **85**, 2523–2527.
- Zulauf, M. & D'Arcy, A. (1992). *J. Cryst. Growth*, **122**, 102–106.